

Critical Currents $I_c(77\text{ K}) > 350\text{ A/cm}$ -Width Achieved in Ex Situ YBCO Coated Conductors Using a Faster Conversion Process

R. Feenstra, A. A. Gapud, F. A. List, E. D. Specht, D. K. Christen, T. G. Holesinger, and D. M. Feldmann

Abstract—Implementation of improved processing for BaF_2 ex situ YBCO coatings from e-beam evaporated precursors enables faster conversion with rates up to 12 \AA/s and critical currents I_c at 77 K greater than 350 A/cm -width on a RABiTS template. Details of the faster processing are described and compared to an earlier slower process. A linear relation between I_c and YBCO layer thickness provides evidence of new opportunities to further improve I_c .

Index Terms— BaF_2 ex situ process, critical currents, thickness dependent effects, vortex pinning, YBCO coated conductors.

I. INTRODUCTION

AS SUGGESTED by the layered geometry, studies to enhance critical currents I_c in $\text{YBa}_2\text{Cu}_3\text{O}_7$ (YBCO) coated conductors (CCs) proceed in two complementary ways. From an established set of growth parameters, a primary approach is to increase the YBCO layer thickness d , recording gains in I_c due to a larger superconductor cross section [1]. Alternatively, for a suitably large value of d , research may focus on increasing the critical current density J_c by process optimization [2]. Latter research may restrict itself to YBCO growth parameter adjustments, or expand into related areas such as interactions with the substrate or defect structures for vortex pinning. Application of the processing adjustments to films of variable thickness tests the general validity of the improvements and sets a framework for cyclical development. With each process iteration, distinct functional dependences of I_c (or J_c) on d provide a touchstone for the underlying physics of layered superconductors [3], while in a practical sense, they provide a gauge to measure the progress.

A physical vapor deposition (PVD) BaF_2 ex situ process for YBCO epitaxial film growth has been under development for CC applications since 1998 [4]. Starting from a “baseline” set of processing parameters, we found consistent $I_c(d)$ relations in the range $0.2 \leq d \leq 3\text{ }\mu\text{m}$ for YBCO coatings on both RABiTS (rolling assisted biaxially textured substrates) and IBAD-YSZ

templates (IBAD: ion-beam assisted deposition) [5]. Recently, efforts have focused on defining new processing parameters to enable faster conversion of the precursor into YBCO. Conversion rates limited to $\sim 1\text{ \AA/s}$ are considered inefficient for scale-up. On the other hand, 10–50 times faster conversion rates have been reported for a close variant of the PVD BaF_2 process, where the precursor layers were produced by metal-organic deposition (MOD) of trifluoroacetate solutions [6], [7]. An enhanced porosity of MOD precursors has been proposed as a possible cause of the rate disparity, by enabling faster diffusion of gaseous reactant (H_2O) and product (HF) species through the precursor layer. However, a complete mechanistic description of the BaF_2 conversion process has not been given, leaving open questions regarding reaction pathways and the order of events. Strong *similarities* in the YBCO structure after conversion have been observed for either precursor type. These structures indicate a laminar growth mechanism, apparently mediated by transient liquid phase formation [8].

Differentiating between “conversion” (chemical process) and “YBCO c-axis epitaxial growth”, we pursued alternative possibilities. While the kinetics of gas exchange likely control certain aspects of the laminar growth, other parameters related to phase formation, such as the reactant microstructure or transitory oxygen concentration, have remained underexposed. Opportunities exist to modify these parameters prior to the high-temperature conversion, as they do spontaneously in the course of heating [9]. Indeed, previous research suggested a connection with the precursor history and such “lineage” was thought to be a cause of residual I_c variability.

This report relates basic features of a newly developed faster conversion process, contrasting it with the baseline process. Implications for I_c are examined. For the first time, width-normalized I_c values that are comparable to commercial Ag-Bi-2223 multi-filamentary composite (MFC) wire [10] were obtained.

II. EXPERIMENTAL DETAILS

The research evaporation chamber used to deposit precursor layers was described in an early publication [11]. Briefly, films of variable thickness d are deposited by simultaneous evaporation from electron-beam Y, BaF_2 , and Cu sources. Composition control is achieved by quartz crystal monitors (QCMs) of the three individual evaporation rates. To avoid BaF_2 excess (within the margins of rate stability), set points are biased toward a small BaF_2 deficiency/Y-excess. Expressed in ratios of the constituents, characteristic values are: $[\text{Y}/\text{Ba}] = 0.55$ and

Manuscript received October 5, 2004. This work was supported by the U.S. Department of Energy under contract DE-AC05-00OR22725 with the Oak Ridge National Laboratory, managed by UT-Battelle, LLC.

R. Feenstra, A. A. Gapud, F. A. List, E. D. Specht, and D. K. Christen are with the Oak Ridge National Laboratory, Oak Ridge, TN 37831 USA (e-mail: feenstrar@ornl.gov).

T. G. Holesinger is with the Los Alamos National Laboratory, Los Alamos, NM 87545 USA (e-mail: holesinger@lanl.gov).

D. M. Feldmann is with the Applied Superconductivity Center, University of Wisconsin, WI 53706 USA (e-mail: feldmann@cae.wisc.edu).

Digital Object Identifier 10.1109/TASC.2005.848217

$[\text{Ba}/\text{Cu}] = 0.60$. This composition is referred to as “stoichiometric”. As part of this work we have also studied effects of Y_2O_3 doping on vortex pinning and thickness dependent trends. These Y-rich films were produced by increasing the Y evaporation rate relative to the Cu and BaF_2 .

During deposition, the substrates were slightly heated to $\sim 100^\circ\text{C}$. Small amounts of O_2 were dosed into the vacuum chamber to (partially) oxidize the deposit and minimize reduction of substrate CeO_2 buffer layers. Setting an appropriate O_2 pressure requires some optimization because extraneous factors such as gettering from freshly deposited Y, chamber cleanliness, pumping speed, etc. can affect the result. Stable precursors with the capacity to convert fast were produced with the O_2 background pressure controlled to stationary values of $(5 - 9) \times 10^{-6}$ Torr, i.e. at an increased level relative to the idling background (2×10^{-6} Torr) or the vacuum without O_2 addition ($\leq 1 \times 10^{-6}$ Torr). Thickness values d were inferred from the combined QCM readings, calibrated against profilometry and Rutherford backscattering spectroscopy measurements after conversion.

RABiTS tapes used in this study were provided by American Superconductor Corporation (AMSC). They feature a $75 \mu\text{m}$ thick Ni-5%W deformation-textured metal template with average grain size of $\sim 25 \mu\text{m}$, and epitaxial Y_2O_3 , YSZ, and CeO_2 buffer layers. Texture parameters measured on the YSZ average: $\Delta\Phi(\text{true}) = 4.8^\circ$ and $\Delta\omega = 5.8^\circ$. Reel-to-reel-produced ORNL RABiTS also was used. $I_c(d)$ data for baseline-processed films on these substrates are compared to fast-processed films on the AMSC template. While a small texture difference skews the comparison somewhat, experiments confirm that conclusions regarding fast vs. baseline processing hold for both templates. The ORNL RABiTS architecture features $50 \mu\text{m}$ thick Ni-3%W metal tape coated with a Ni overlayer, and Y_2O_3 , YSZ, CeO_2 buffer layers. Average texture parameters for the YSZ are: $\Delta\Phi(\text{true}) = 6.1^\circ$ and $\Delta\omega = 5.5^\circ$. Prior to mounting in the precursor deposition chamber, the substrates were annealed in flowing N_2 gas (containing < 80 ppm O_2) to temperatures in the range $700\text{--}750^\circ\text{C}$ for 0.5 h.

Ex situ conversion was performed in either of two annealing systems. The majority of films were processed in the standard tube furnace described in [11], equipped to operate with flowing gas mixtures at atmospheric pressure. Relatively large flow rates corresponding to a plug-flow velocity of 4 m/min were used. Helium served as the carrier gas. Improvements in the gas handling system allow for a flexible range of water partial pressures, from dilute (calculated dew point $< -30^\circ\text{C}$) to concentrated (~ 0.1 atm). The O_2 partial pressure was set at 250 ppm.

A second conversion system, equipped with in situ XRD capability and operating at reduced absolute pressures, was used to study conversion rates for films of a fixed $1 \mu\text{m}$ thickness. Details of this system were recently described by List *et al.* [12]. Annealing was performed in (Ar , O_2 , H_2O) gas mixtures at total pressures of 0.5–2.5 Torr and O_2 partial pressure of 200 mTorr. Sample dimensions for the two furnace systems reflect systemic differences in out-flow capacity. This capacity is enhanced and more homogeneously distributed at sub-atmospheric operating pressures. Design sample dimensions for the low-pressure conversion system are: $3 \text{ cm} \times 1 \text{ cm}$. Precursor areas reduced by a

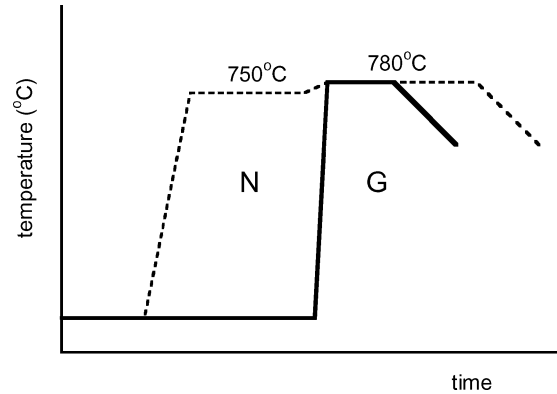


Fig. 1. Schematic temperature-time diagram of the “fast” conversion process (solid) and the “baseline” process (dashed) in the standard 1-atm furnace system. In the baseline process, a 0.5–1 h nucleation step (N) at reduced water supply (0.04–0.2%) precedes the main “growth” annealing step (G) at optimized water concentration of $\sim 0.5\%$ (relative to 1 atm). The fast process bypasses the N-step via a fast ramp and provides an increased water supply (1–2%). An oxidation step at 500°C followed by slow cooling (not shown) concludes both processes.

factor of 10 were used for fast conversion in the standard 1-atm system. Narrow precursor strips ~ 2 mm wide were deposited onto 1.5 cm long \times 5 mm wide substrates through a shadow mask. XRD after the high-temperature anneal confirmed that full conversion of similarly thick precursors could be achieved in both systems using similar annealing times.

Transport critical currents were measured using a standard four-probe technique and $1 \mu\text{V}/\text{cm}$ criterion. Measurements were made over the full YBCO width. Where current limitations prevented determination of the self-field I_c , values were extrapolated from measurements in applied magnetic fields $H \parallel c$, using lower- I_c , thin films for calibration. That this procedure should lead to consistent results as a function of d is not obvious. However, as reported elsewhere in more detail [13], consistency is confirmed by a high degree of uniformity in the H-field dependence for variable thickness films (made with the ex situ process), described by a power law $J_c \propto H^{-\alpha}$ in the range 0.1–1 T with narrow distribution of exponents $\alpha \cong 0.6$. These observations add confidence to the robustness of observed I_c enhancements, as they occur over a substantial H field range.

III. FAST CONVERSION PROCESS

A schematic temperature-time diagram for the fast process (1 atm conversion system) is shown in Fig. 1, contrasting it to the baseline process. Fast conversion was achieved by heating the precursor at a rate of $130^\circ\text{C}/\text{min}$ to $\sim 780^\circ\text{C}$ in gas mixtures containing 1–2% water vapor. The annealing duration was computed from a presumed growth rate and the film thickness. Following conversion, the water supply is turned off, starting a drying time of 3 min, prior to cooling. Excluding the drying time, annealing durations corresponding to growth rates of 5–12 $\text{\AA}/\text{s}$ were found to produce complete conversion into YBCO for thickness values ranging from 0.2–2 μm . Electrical resistivity values at room temperature were in the range 200–300 $\mu\Omega\cdot\text{cm}$.

A direct confirmation of the conversion rate is provided by the in situ XRD data of Fig. 2 (low-pressure system). Indicated are time dependent, normalized peak intensities of BaF_2 (111) and

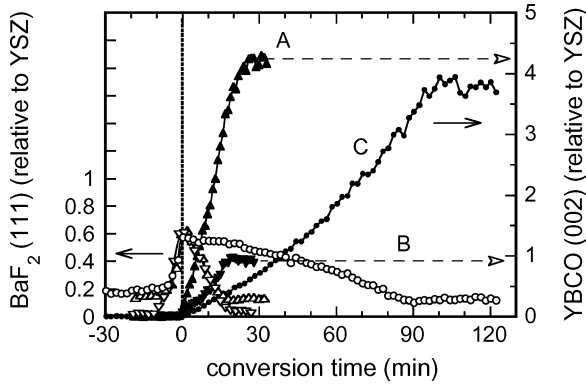


Fig. 2. Time dependent variations of the peak intensities of BaF_2 (111) (open symbols, left axis) and YBCO (002) (closed symbols, right axis) reflections during fast (samples A, B) and baseline (sample C) conversion processes. The zero point of conversion time is defined as the moment that the sample temperature reaches the set point.

YBCO (200) reflections for three $1 \mu\text{m}$ thick films (A, B, C) during the conversion process. Fast-conversion processing parameters were used for samples A and B. These parameters include a temperature of 780°C , water pressure of 5 mTorr and an absolute total pressure of 0.5 Torr. Behavior typical of the baseline process is illustrated by sample C. Parameters were set according to a previous optimization study [12] to an absolute pressure of 2.5 Torr, 740°C , and 5 mTorr water pressure. A short anneal (0.5 h) at 400°C in 0.1 atm O_2 applied to samples A and C prior to ex situ conversion provides further differentiation. Such an anneal is not part of the standard protocol for PVD BaF_2 precursors, however, it was added here to increase the average oxidation level and/or modify the microstructure. Evidence of structural changes may be inferred from the appearance of weak BaF_2 reflections in the $\theta - 2\theta$ XRD spectrum. By contrast, sample B was converted directly from the as-deposited state.

Disappearance of the BaF_2 signal and saturation of the YBCO intensity occur simultaneously and mark the moment at which conversion is complete. Thus, it is seen that the annealing duration for the fast sample (A) is reduced by a factor of ~ 4.5 compared to the slower conversion (sample C), from 90 to about 20 min. The corresponding growth rate is $\sim 9 \text{ \AA/s}$. The primary cause of faster conversion for sample A stems from the imposed “aggressive” conversion parameters, featuring a higher temperature and reduced absolute pressure. Although the water supply was kept constant, the reduced total pressure increases the chemical driving force for BaF_2 decomposition by increasing the HF removal rate. Note that for both samples the YBCO saturation level is well developed and reaches a similar intensity.

A very different picture is provided by sample B, converted with fast-conversion parameters but without the intermediate anneal. While the BaF_2 intensity shows the same time dependence as A (indicating that fast conversion did occur), the c-axis YBCO signal remains low, and levels off after about 20 min. A full XRD $\theta - 2\theta$ spectrum shows that this film had grown to a structure with multiple YBCO orientations, characterized by weak (00L) reflections. I_c of this film reached merely 0.1 A at 77 K. By contrast, only (00L) reflections were measured for the properly converted film A, yielding a high I_c value of

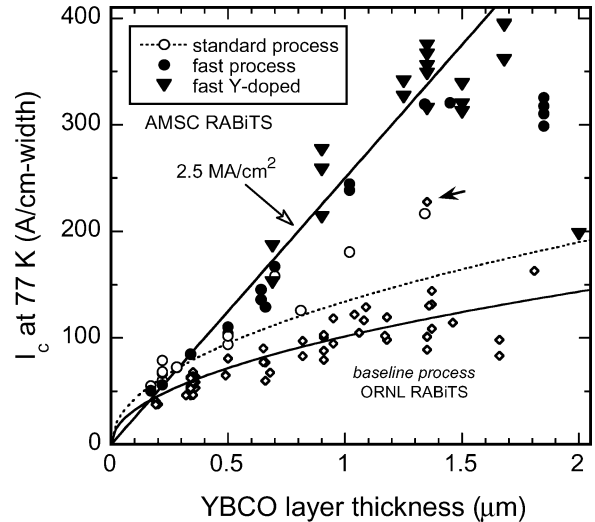


Fig. 3. Variation of the critical current I_c normalized to 1-cm width with layer thickness d of *ex situ* processed YBCO coatings on RABiTS templates. The films were converted from PVD BaF_2 precursors. Fast-processed samples are indicated by the solid symbols. The straight line was calculated for a constant J_c of 2.5 MA/cm^2 . Curves through the baseline (standard) process data represent trend lines according to: $I_c = I_c(1)d^{1/2}$ where d is in μm . $I_c(1) = 134 \text{ A/cm}$ for AMSC RABiTS (standard process) and 101 A/cm for ORNL RABiTS (baseline process). An exceptional film on ORNL RABiTS ($d = 1.34 \mu\text{m}$) described in [8] is highlighted with a small arrow.

189 A/cm-width. Modifications introduced by the intermediate anneal for A improved the c-axis epitaxial growth mechanism for the same conversion rate. This feature stands out as the primary benefit of the intermediate anneal.

Within the larger context of this research, the disparity between samples A and B qualifies as extreme. It is clear, however, that the precursor preparation history enters into the conversion process. Experimentation with inserted modification anneals was started in studies of the baseline process, where they revealed contradictory but mostly beneficial effects. In a way that is reminiscent of supersaturation in epitaxial film growth, a large chemical driving force for BaF_2 conversion seems to magnify the role of details in precursor and substrate properties. The procedural step of inserting a low temperature anneal resembles the use of a calcination anneal for MOD BaF_2 precursors. The primary function of this heat treatment, however, is removal of carbon containing residues from the solution-based deposition process and the parameters are optimized to perform this function. The low-temperature annealing conditions selected here for PVD- BaF_2 precursors resulted from preliminary tests covering a relatively small part of parameter space. By expanding the search, we expect that further optimization is feasible. Concurrent adjustments in the ex situ conversion parameters may be needed, however, expanding the optimization matrix. All films described in the remainder of this work featured the intermediate anneal and the temperature-time profile of Fig. 1 for processing at 1.0 atm total pressure.

IV. RELATIONSHIP BETWEEN YBCO THICKNESS AND I_c

Values of $I_c/\text{unit width}$ at 77 K for fast-processed YBCO on AMSC RABiTS are plotted as a function of d in Fig. 3. Two sets of fast-processed films are represented, indicated by

the different (closed) symbols. Initial research focused on stoichiometric (slightly Ba deficient) films. Fig. 3 compares films produced with the fast process (closed circles) to ones produced with a baseline-process variant (open circles, labeled as “standard” process). Starting from $I_c \cong 50$ A/cm for 0.2 μm thick films, I_c increases approximately linearly with d to ~ 320 A/cm for a 1.34 μm thick film. This idealized behavior contrasts with the saturation-like thickness dependence of standard-processed films. Latter behavior is illustrated more clearly by the larger dataset for baseline-processed films on the ORNL template (open diamonds). For thickness values to 3 μm , the trend is suitably described by a square root function of d : $I_c \propto d^{1/2}$. That is, J_c decreases as $1/d^{1/2}$. Other functional forms can provide equally satisfactory representations, such as the type $J_c \propto \exp(-d/d_0) + J_S$ (d_0 and J_S : constants) introduced by Foltyn *et al.* [1] for YBCO films grown by in situ pulsed laser deposition (PLD). Indeed, a remarkable correspondence exists between the trends on a relative scale for this (baseline) ex situ BaF_2 process and in situ PLD. Further discussions of these similarities are deferred to a future publication.

In an attempt to further improve flux pinning properties in the fast-processed films, we initiated a study of the effects from Y-rich compositions. This approach was based on observations by TEM that a high density of Y_2O_3 precipitates of suitably small dimensions (15–50 nm) may be incorporated as inclusions in the laminar YBCO grain structure [8]. Initial studies were performed for films of a fixed thickness of 0.7–0.9 μm . Variations in the Y excess ranged from 30–90%. Results from measurements of J_c as a function of applied magnetic field, temperature, and field orientation are reported in a companion paper at this conference [13]. These studies revealed systematic trends due to Y addition, with self-field J_c increasing and the magnitude of field-angle dependent J_c variations *decreasing*. The data suggest a homogenized flux pinning mechanism due to correlated defects or strain, with a multitude of orientation vectors.

The Y additions also resulted in larger I_c values for films with $d > 0.9$ μm . $I_c > 350$ A/cm was reached for several 30% Y-rich 1.34 μm thick films. Best I_c values to date are ~ 393 A/cm for two 50% Y-rich 1.7 μm thick films. There is an indication that the linear $I_c(d)$ relationship may be extended by increasing the Y doping in thicker films. However, J_c values for the 1.7 μm films fall slightly below the 2.5 MA/cm² trend line as I_c tends to roll over for $d \geq 1.5$ μm . A stagnation in I_c is found for stoichiometric films between $d = 1.35$ μm and 1.85 μm , giving way to a sudden drop in I_c for thicker films. The 2 μm film shown in Fig. 3 contained 90% Y-excess. I_c continues to decrease for thicker films (not shown) to values less than extrapolated from the baseline square root dependence, indicating that developed fast-processing conditions are not optimal for this thickness range. Within the linear regime, however, the realized gains are substantial. Maximum I_c values are equivalent to those reported for first-generation Ag-Bi-2223 MFC tape. Previous equivalent performance levels featured relatively thick YBCO coatings ($d \geq 3$ μm) produced by PLD on highly textured IBAD templates [14], [15]. The present results show that application-grade conductors are now also available from a BaF_2 ex situ process.

According to the basic definition $I_c/w = J_c d$, a linear relationship between I_c per cm-width (w) and layer thickness

d results if J_c remains constant. Because of the difficulty in sustaining a self-replicating growth process in YBCO epitaxial films, it might be expected that strongly processing and substrate dependent effects on J_c , would render this an unlikely scenario. With the fast process, however, “constant” J_c values of 2.3–2.7 MA/cm² are obtained for all thickness values in the range 0.17–1.7 μm .

The origin of this near-ideal behavior remains under investigation. A linear $I_c(d)$ relation previously was obtained upon thinning (by ion milling) of thick ex situ YBCO coatings (0.9–2.9 μm) on ORNL RABiTS and IBAD-YSZ templates [16]. These baseline-processed films, however, contained “bimodal” laminar structures, with large YBCO grains near the substrate, intercalated Ba-rich secondary phases, and smaller YBCO grains near the surface [8]. A change in the growth mechanism midway through the precursor as the conversion proceeds, appears inconsistent with the observed, nearly constant J_c through thickness, perhaps pointing to compensating effects.

Preliminary results from TEM and XRD texture analysis suggest that the onset of bimodal growth (as a function of thickness) is delayed to $d > 1.3$ μm for fast-converted films. Indeed, a homogeneous, nonbimodal microstructure was observed by TEM for one of the 1.25 μm thick Y-rich films shown in Fig. 3 with $I_c \cong 340$ A/cm. This film displayed a complete absence of interface reactions with the CeO_2 buffer layer. Contrary to the linear $I_c(d)$ relation in the ion milling study, the linear dependence for these variable thickness, fast-processed films ($d < 1.3$ μm), therefore, could be the result of an invariant microstructure. However, as we discuss next, additional structural trends do occur.

Behavior indicative of bimodal growth was observed for one of the 1.85 μm films ($I_c \cong 320$ A/cm). Using through-thickness ion milling along with electron backscatter Kikuchi pattern (EBKP) analysis, we find that the introduction of additional grain boundary (GB) networks in the top part of the film is likely related to the sudden decrease in I_c for this film and others of larger thickness. Future research is directed at improving this undesirable behavior.

More generally, the EBKP imaging as well as cross section TEM, provide evidence of complex GB structures in these ex situ films. This is related to a tendency of the YBCO to completely or partially overgrow substrate GBs, which depends on the thickness. Films in the ~ 1 μm range are especially rich in their characteristics. YBCO GBs for this thickness are found to “meander” about the projected substrate GB plane, both through the thickness and parallel to the substrate surface. A companion paper describes these observations in more detail [17]. The role of curved and tilted GB planes on supercurrent transmission is practically undocumented and is being studied via newly initiated bi-crystal experiments. These hidden complexities attest to the fact that even if seemingly ideal behavior is observed, the physical mechanisms underlying current transport in YBCO CCs are still incompletely understood.

V. SUMMARY

A faster conversion process of PVD BaF_2 precursors has been described with the ability to produce c-axis YBCO at rates

up $\sim 12 \text{ \AA/s}$, both in a standard, 1-atm furnace and at reduced absolute pressures. A low-temperature oxidation anneal, inserted as an extra processing step between precursor deposition and ex situ conversion enables application of aggressive conversion conditions. Fast converted films exhibit a linear relationship between J_c and the YBCO layer thickness d in the range $0.2\text{--}1.7 \text{ }\mu\text{m}$. Enhanced vortex pinning properties and self-field J_c resulted from Y doping over a similar thickness range. Best J_c values of $\sim 400 \text{ A/cm}$ (77 K) are equivalent to the performance of industrially produced Ag-Bi-2223 wire.

Finally, we note that significantly larger J_c values of $\sim 3.4 \text{ MA/cm}^2$ were recently reported by AMSC for $0.8 \text{ }\mu\text{m}$ thick ex situ YBCO converted from MOD precursors over 10-m production lengths on RABiTS tape similar to the tapes supplied to us [18]. Extension of these high J_c values to the $1.5\text{--}2 \text{ }\mu\text{m}$ range appears feasible based on the present results, raising the prospect of conductors with drastically improved price-to-performance ratio.

REFERENCES

- [1] S. R. Foltyn, Q. X. Jia, P. N. Arendt, L. Kinder, Y. Fan, and J. F. Smith, "Relationship between film thickness and the critical current of YBCO coated conductors," *Appl. Phys. Lett.*, vol. 75, p. 3692, 1999.
- [2] M. W. Rupich *et al.*, "YBCO coated conductors by an MOD/RABiTS process," *IEEE Trans. Appl. Supercond.*, vol. 13, p. 2458, 2003.
- [3] A. Gurevich, "Thickness Dependence of Critical Currents in Thin Superconductors," . manuscript in preparation.
- [4] R. Feenstra, "The BaF_2 method: a scalable process for YBCO coated conductors," presented at the *US Dept of Energy Wire Development Workshop*, St. Petersburg, FL, Jan. 29–30, 1998.
- [5] R. Feenstra, T. G. Holesinger, and D. M. Feldmann, "Materials and intrinsic properties in the J_c dependence on thickness of ex situ YBCO coated conductors," presented at the *US Dept of Energy Superconductivity for Electric Systems 2003 Annual Review*, Washington DC, July 23–25, 2003.
- [6] M. Yoshizuma, I. Seleznev, and M. J. Cima, . manuscript in preparation.
- [7] F. A. List, P. G. Clem, L. Heatherly, J. T. Dawley, K. J. Leonard, D. F. Lee, and A. Goyal, "Low-Pressure Conversion Studies for YBCO Precursors Derived by PVD and MOD Methods," in *this conference*.
- [8] T. G. Holesinger, P. N. Arendt, R. Feenstra, A. A. Gapud, E. D. Specht, D. M. Feldmann, and D. C. Larbalestier, "Liquid mediated growth and the bi-modal microstructure of YBCO films made by ex situ conversion of PVD- BaF_2 precursors," *J. Mater. Res.*, 2004, submitted for publication.
- [9] W. Wong-Ng, I. Levin, R. Feenstra, L. P. Cook, and M. Vaudin, "Phase evolution of YBCO films during the BaF_2 process," *Supercond. Sci. & Technol.*, vol. 17, p. S548, 2004.
- [10] Y. B. Huang *et al.*, "Improving the critical current density in Bi-2223 wires via a reduction of the secondary phase content," *IEEE Trans. Appl. Supercond.*, vol. 13, p. 3038, 2003.
- [11] R. Feenstra, T. B. Lindemer, J. D. Budai, and M. D. Galloway, "Effect of oxygen pressure on the synthesis of YBCO thin films by post-deposition annealing," *J. Appl. Phys.*, vol. 69, p. 6569, 1991.
- [12] F. A. List, E. D. Specht, L. Heatherly, K. J. Leonard, S. Sathyamurthy, and D. M. Kroeger, "Crystalline phase development during vacuum conversion of thin barium fluoride precursor films on metallic substrates," *Physica C*, vol. 391, p. 350, 2003.
- [13] A. A. Gapud, R. Feenstra, D. K. Christen, J. R. Thompson, and T. G. Holesinger, "Temperature and Magnetic Field Dependence of Critical Currents in YBCO Coated Conductors With Processing-Induced Variations in Pinning Properties," . presented at *this conf.*
- [14] S. R. Foltyn *et al.*, "Strongly coupled critical current density values achieved in YBCO coated conductors with near-single-crystal texture," *Appl. Phys. Lett.*, vol. 82, p. 4519, 2003.
- [15] A. Usoskin, H. C. Freyhardt, A. Issaev, and J. Knoke, "YBCO coated conductors with extra-high engineering current densities and their implementation in power engineering," presented at the *Fall Meeting of the Mater. Res. Soc.*, Dec. 1–4, 2003.
- [16] D. M. Feldmann, D. C. Larbalestier, R. Feenstra, A. A. Gapud, J. D. Budai, T. G. Holesinger, and P. N. Arendt, "Through-thickness superconducting and normal-state transport properties revealed by thinning of thick film ex situ YBCO coated conductors," *Appl. Phys. Lett.*, vol. 83, p. 3951, 2003.
- [17] D. M. Feldmann, D. C. Larbalestier, R. Feenstra, and T. G. Holesinger, "Large Grains and Substrate Grain Overgrowth Resulting From Liquid-Mediated YBCO Growth in Coated Conductors," . manuscript in preparation.
- [18] A. P. Malozemoff, M. W. Rupich, and U. Schoop, "Scale-up of coated conductor technology at american superconductor," in *Superconductivity for Electric Systems 2004 Annual Review*, Washington DC, July 27–29, 2004.